Iterative Block Decision Feedback Equalization for MIMO Underwater Acoustic Communications

Jun Tao[†], Yahong Rosa Zheng[§], Chengshan Xiao[§], T. C. Yang[‡]

[†]Dept. of Electrical & Computer Eng., University of Missouri, Columbia, MO 65211, USA

[§]Dept. of Electrical & Computer Eng., Missouri University of Science & Technology, Rolla, MO 65409, USA

[‡]Naval Research Laboratory, Washington, DC 20375, USA

***Abstract*— A new receiver design using iterative block decision-feedback equalizer (BDFE) is proposed for high data rate single-carrier multiple-input, multiple-output (MIMO) underwater acoustic (UWA) communications. The adoption of BDFE enables a *sequence-based* log-likelihood ratio (LLR) calculation during iterative equalization, thus leading to better performance and faster convergence than existing low-complexity iterative equalization methods using *symbol-based* LLR evaluation. The proposed BDFE method is applied to overlapped blocks to reduce performance degradation at the tail of each block. The block size is flexibly selected depending on the practical channel condition. The proposed receiver scheme has been tested by extensive experimental data and proved to be robust to different transmission environments with consistently good detection performance. Data from collected during the SPACE08 experiment near Martha's Vineyard and the GOMEX08 experiment at the Gulf of Mexico, are both presented here.**

I. Introduction

Underwater acoustic (UWA) communications are challenging for three main reasons: first, the available channel bandwidth is very limited due to frequency-dependent attenuation; second, the multi-path delay spread is excessively long; third, the Doppler spread effect is significantly large. Due to the harsh channel condition, demonstrated rates in UWA communications are limited to several kilo-bits per second within 40 km range. Multiple-input, multiple-output (MIMO) communications which improve the data rate significantly by employing parallel independent propagation channels existing in the ocean, however, are much harder than single-input, multiple-output (SIMO) communications due to not only the inter-symbol interference (ISI) but also the multi-access interference (MI) from signals other than the desired signal.

Many approaches have been proposed for UWA receiver designs. Earlier UWA systems have used non-coherent frequency-shift keying (FSK). Bandwidth and power efficient coherent modulation scheme has been first developed in early 1990's [1]. In recent years, much progress has been made [2]–[7] in coherent UWA communications. The frequency-domain (FD) designs using single-carrier frequency-domain equalization (SC-FDE) and orthogonal frequency division multiplexing (OFDM), are found in [2] and [3], [4], respectively. The time-domain (TD) receiver designs using channel equalization are found in [5] and [6], [7] using MIMO technology. The advantage of the TD designs is that no gaps are inserted among transmission blocks, resulting in higher data efficiency over common FD block transmission methods.

The advent of iterative equalization technology [8] has enabled powerful receiver design. The iterative equalization for UWA communications has been first proposed in [9] with a joint maximum *a posteriori* probability (MAP) iterative equalizer and turbo decoder. However, the complexity of MAP equalizer is prohibitively high, and a low-complexity iterative decision-feedback equalizer (DFE) has been proposed and tested by a multichannel UWA transmission [10]. Iterative DFE for MIMO systems has been proposed in [7], using a multi-band transmission. Iterative equalization using linear equalizer (LE) [11] has also been applied to UWA communications [12], [13], with extensive experimental tests demonstrating the effectiveness of the iterative LE scheme.

Hard-decision block decision-feedback equalizer (BDFE), which performs better in fast time-varying multi-path channel than its conventional DFE counterpart, has been proposed in [14], and soft-decision iterative BDFE has been proposed in [16], both for single-input single-output (SISO) systems. In this paper, we develop an iterative BDFE for MIMO systems and apply it to high-rate UWA communications. The proposed MIMO BDFE performs successive interference cancelation (SIC) of both ISI in the time domain and MI in the space domain. It enables a near-optimum *sequence-based* log-likelihood ratio (LLR) evaluation, which is superior to the conventional *symbol-based* LLR calculations. The proposed receiver design is tested by extensive experimental data collected at the Martha's Vineyard, Edgartown, MA, in October 2008, and at the Gulf of Mexico, in July 2008.

II. System Model

Consider a MIMO UWA system with N transducers and M hydrophones, shown in Fig. 1, where $a_{n,k}$ denoting the k-th bit of the n-th stream, is encoded, interleaved, and modulated, into $b_{n,k}$, $c_{n,k}$, and $s_{n,k}$. The modulated symbols, $s_{n,k}$, are formatted for transmission. For the system employing a constellation of size Q, the group of coded bits, $\{c_{n,(k-1)\log_2 Q+p}\}_{p=1}^{\log_2 Q}$, are mapped to the modulation symbol $s_{n,k}$.

The baseband signal received at the m-th hydrophone is expressed by

$$y_{m,k} = \sum_{n=1}^{N} \sum_{l=0}^{L-1} h_{n,m}(k,l) s_{n,k-l} + v_{m,k} \tag{1}$$

where $h_{n,m}(k,l)$ is the l-th fading coefficient between the n-th transducer and the m-th hydrophone at time k.

0-933957-38-1 ©2009 MTS

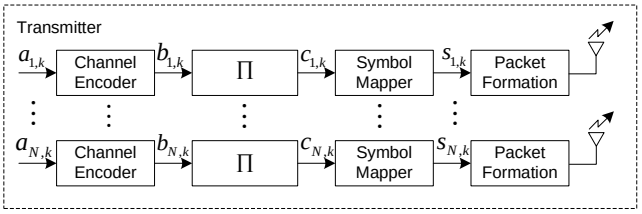

Fig. 1. MIMO transmitter.

III. Iterative MIMO Receiver

The structure of the proposed iterative MIMO receiver is depicted in Fig. 2, where the soft-decision MIMO BDFE iteratively exchanges soft decisions with MAP decoders, through the interleavers ($\prod$) and the de-interleavers ($\prod^{-1}$). The MIMO BDFE is performed jointly for M received streams to yield N soft-decision streams $\{\Lambda(c_{n,k})\}_{n=1}^{N}$. The soft decisions, with the *a priori* soft decisions being subtracted out, are delivered through the de-interleavers for MAP decoding. The MAP decoders generate new soft decisions, $\{\Lambda^D(b_{n,k})\}_{n=1}^{N}$, about coded bits. The new soft streams, with the *a priori* soft decisions being subtracted out, are fed back through the interleavers for equalization. Detection performance is gradually improved over iterations and the final hard decisions $\{\hat{a}_{n,k}\}_{n=1}^{N}$ are made after convergence.

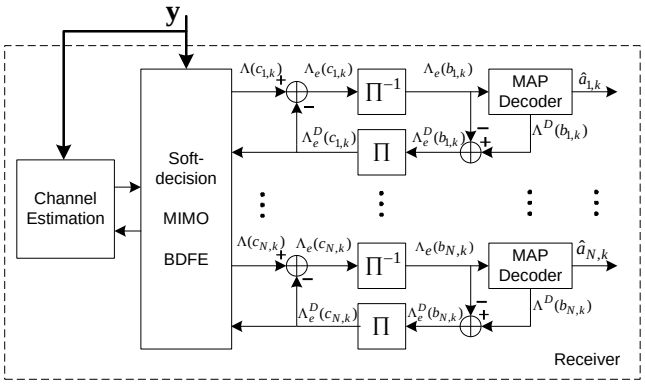

Fig. 2. Iterative receiver using soft-decision MIMO BDFE.

A. Soft-decision MIMO-BDFE

Consider a length-K symbol block, $\mathbf{s}_n = [s_{n,1}, \cdots, s_{n,K}]^t \in \mathcal{S}^{K\times 1}$, where $(\cdot)^t$ denotes matrix transpose and $\mathcal{S} = \{\chi_q\}_{q=1}^{Q}$ is the constellation set with cardinality Q. Within each block, the channel is treated as time-invariant [14]. Defining received signal vector $\mathbf{y}_m = [y_{m,1}, y_{m,2}, \cdots, y_{m,K}]^t$, additive noise vector $\mathbf{v}_m = [v_{m,1}, v_{m,2}, \cdots, v_{m,K}]^t$ for the m-th hydrophone and stacking up $\{\mathbf{y}_m\}_{m=1}^{M}$, $\{\mathbf{v}_m\}_{m=1}^{M}$ and $\{\mathbf{s}_n\}_{n=1}^{N}$ into column vectors leads to

$$\mathbf{y} = \mathbf{H}\mathbf{s} + \mathbf{v} \tag{2}$$

where $\mathbf{H} \in \mathcal{C}^{MK\times NK}$ is a block matrix with the (m,n)-th block being channel matrix $\mathbf{H}_{m,n}$ defined as

$$\mathbf{H}_{m,n} = \begin{bmatrix} h_{m,n}(0) & 0 & 0 & \cdots & 0 \\ h_{m,n}(1) & h_{m,n}(0) & 0 & \cdots & 0 \\ \vdots & \ddots & \ddots & \ddots & \vdots \\ 0 & \cdots & h_{m,n}(L-1) & \cdots & h_{m,n}(0) \end{bmatrix}. \tag{3}$$

The soft-decision MIMO-BDFE performs detection of the k-th symbol from the n-th data stream, $s_{n,k}$, through a feedforward filter, $\mathbf{W}_{n,k} \in \mathcal{C}^{NK\times MK}$, and a zero-diagonal upper triangular feedback filter, $\mathbf{B}_{n,k} \in \mathcal{C}^{NK\times NK}$, as shown in Fig. 3. The equalized symbol vector before LLR evaluation

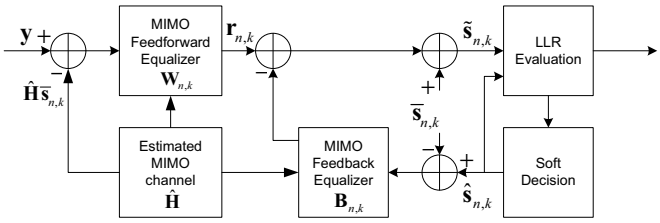

Fig. 3. Soft-decision MIMO-BDFE ($\mathbf{W}_{n,k}$ and $\mathbf{B}_{n,k}$ are the feedforward and feedback MIMO equalizer matrices when the k-th symbol of the n-th stream is equalized.)

can be written as

$$\tilde{\mathbf{s}}_{n,k} = \mathbf{W}_{n,k}(\mathbf{y} - \mathbf{H}\bar{\mathbf{s}}_{n,k}) - \mathbf{B}_{n,k}(\hat{\mathbf{s}} - \bar{\mathbf{s}}_{n,k}) + \bar{\mathbf{s}}_{n,k} \tag{4}$$

where the estimated channel $\hat{\mathbf{H}}$ in Fig. 3 is replaced by the true channel $\mathbf{H}$ for the convenience of denotation, and $\bar{\mathbf{s}}_{n,k}$ is obtained by setting the mean of $s_{n,k}$ in the mean vector $\bar{\mathbf{s}} \triangleq \mathbb{E}[\mathbf{s}]$ to zero while leaving all the other elements unchanged. The operation $\mathbb{E}[\cdot]$ denotes mathematical expectation. The employment of $\bar{\mathbf{s}}_{n,k}$ instead of $\bar{\mathbf{s}}$ is to avoid the instability caused by positive feedback. The vector $\hat{\mathbf{s}} = [\hat{s}_{1,1}, \cdots, \hat{s}_{1,K}, \cdots, \hat{s}_{N,1}, \cdots, \hat{s}_{N,K}]^t \in \mathcal{C}^{NK\times 1}$ contains the soft-decision symbols.

With the common assumption of perfect decision feedback, *i.e.*, $\hat{\mathbf{s}} = \mathbf{s}$, the error vector of BDFE can be written as

$$\mathbf{e}_{n,k} = \mathbf{W}_{n,k}(\mathbf{y} - \mathbf{H}\bar{\mathbf{s}}_{n,k}) - (\mathbf{B}_{n,k} + \mathbf{I}_{NK})(\mathbf{s} - \bar{\mathbf{s}}_{n,k}) \tag{5}$$

where $\mathbf{I}_{NK}$ is an identity matrix of size NK. Minimizing the mean square error, $\mathbb{E}\left[\mathbf{e}_{n,k}^h \mathbf{e}_{n,k}\right]$, leads to the solutions for the feedforward and feedback matrices

$$\mathbf{B}_{n,k} = \mathbf{G}_{n,k} - \mathbf{I}_{NK}, \tag{6a}$$

$$\mathbf{W}_{n,k} = \mathbf{G}_{n,k}\mathbf{\Phi}_{n,k}\mathbf{H}^h \left[\mathbf{H}\mathbf{\Phi}_{n,k}\mathbf{H}^h + \sigma_v^2 \mathbf{I}_{NK}\right]^{-1} \tag{6b}$$

where $(\cdot)^h$ denotes matrix conjugate transpose, $\mathbf{\Phi}_{n,k}$ is obtained by setting the variance of $s_{n,k}$ in the covariance matrix, $\mathbf{\Phi} \triangleq \mathbb{E}\left[(\mathbf{s} - \bar{\mathbf{s}})(\mathbf{s} - \bar{\mathbf{s}})^h\right]$ as one, and $\mathbf{G}_{n,k} \in \mathcal{C}^{NK\times NK}$ is an unit-diagonal upper triangular matrix obtained from the Cholesky decomposition of $\mathbf{\Phi}_{n,k}^{-1} + \frac{1}{\sigma_v^2}\mathbf{H}^h\mathbf{H}$ as

$$\mathbf{\Phi}_{n,k}^{-1} + \frac{1}{\sigma_v^2}\mathbf{H}^h\mathbf{H} = \mathbf{G}_{n,k}^h \mathbf{D}_{n,k} \mathbf{G}_{n,k} \tag{7}$$

with $\mathbf{D}_{n,k} \in \mathcal{C}^{NK\times NK}$ being a diagonal matrix. With the filters in (6), the original system is converted to an equivalent system as (c.f. (5))

$$\mathbf{r}_{n,k} \triangleq \mathbf{W}_{n,k}\left(\mathbf{y}-\mathbf{H}\bar{\mathbf{s}}_{n,k}\right) = \mathbf{G}_{n,k}\left(\hat{\mathbf{s}}-\bar{\mathbf{s}}_{n,k}\right)+\mathbf{e}_{n,k}. \quad (8)$$

B. Sequence-based LLR Calculation

In the i-th iteration, the *sequence-based a posteriori* probability (APP) of $s_{n,k}^{(i)}$ conditioned on $\mathbf{r}_{n,k}$ is

$$P\left(s_{n,k}^{(i)}|\mathbf{r}_{n,k}\right) = \frac{P\left(\mathbf{r}_{n,k}|s_{n,k}^{(i)}\right)P\left(s_{n,k}^{(i)}\right)}{p\left(\mathbf{r}_{n,k}\right)}. \quad (9)$$

Based on the assumption that $\mathbf{e}_{n,k}$ in (8) is a random vector with independent Gaussian elements, we can simplify the probability calculation as

$$P\left(\mathbf{r}_{n,k}|s_{n,k}^{(i)}\right) \approx \prod_{j=1}^{NK}\frac{1}{\pi\sigma_j}\exp\left\{-\frac{\left|\rho_{n,k}^{j}\right|^2}{\sigma_j^2}\right\} \quad (10)$$

where $\sigma_j^2 = d_{j,j}^{-1}$ with $d_{j,j}$ being the j-th diagonal element of $\mathbf{D}_{n,k}$, and $\rho_{n,k}^{j}$ is defined in (11) at the top of the next page. In (11), $g_{j,l}$ is the (j,l)-th element of $\mathbf{G}_{n,k}$, r_j is the j-th element of $\mathbf{r}_{n,k}$, $J=(k-1)N+n$, and the operations $p(l)\triangleq\lceil l/K\rceil$ and $q(l)\triangleq l-(\lceil l/K\rceil-1)K$ represent the mapping from the linear index set, $\{l\}_1^{NK}$, to the double index set, $(p,q)_{(1,1)}^{(N,K)}$. The tentative soft decisions $\hat{s}_{p,q}^{(i-1)}$ and $\hat{s}_{p,q}^{(i)}$ are taken from the $(i-1)$-th iteration and the i-th iteration, respectively. The upper triangular structure of $\mathbf{G}_{n,k}$ determines that the symbols, $s_{p,q}$, with index satisfying $(p-1)K+q > (n-1)K+k$, are detected before $s_{n,k}$, thus the tentative detections of those symbols from the current iteration can be used. The probabilities $P\left(s_{n,k}^{(i)}\right)$ and $p(\mathbf{r}_{n,k})$ are determined by the *a priori* probabilities of mapping bits, and the normalization $\sum_{q=1}^{Q}P\left(s_{n,k}^{(i)}=\chi_q|\mathbf{r}_{n,k}\right)=1$, respectively. With $P\left(s_{n,k}^{(i)}|\mathbf{r}_{n,k}\right)$, the soft-decision symbols can be calculated, and the APP and LLR of the mapping bits, are evaluated as follows

$$P\left[c_{n,(k-1)\log_2 Q+p}^{(i)}=b|\mathbf{r}_{n,k}\right] = \sum_{s_{n,k}^{(i)}\in\mathcal{S}_p^{(b)}}P\left(s_{n,k}^{(i)}|\mathbf{r}_{n,k}\right) \quad (12)$$

$$\Lambda\left[c_{n,(k-1)\log_2 Q+p}^{(i)}\right] = \ln\frac{\sum_{s_{n,k}^{(i)}\in\mathcal{S}_p^{(0)}}P\left(s_{n,k}^{(i)}|\mathbf{r}_{n,k}\right)}{\sum_{s_{n,k}^{(i)}\in\mathcal{S}_p^{(1)}}P\left(s_{n,k}^{(i)}|\mathbf{r}_{n,k}\right)}. \quad (13)$$

where $\mathcal{S}_p^{(b)} \triangleq \{\chi_q|\chi_q\in\mathcal{S}: c_{q,p}=b\}$ with $b\in\{0,1\}$, and $p=1,\cdots,\log_2 Q$. The *a priori* LLR is subtracted from (13) to produce extrinsic LLR for MAP decoders.

C. Low-complexity Approximate Soft-decision MIMO-BDFE

The major computational burden of the proposed iterative equalization comes from the requirement of updating the filter matrices $\mathbf{W}_{n,k}$ and $\mathbf{B}_{n,k}$ for each symbol. In each updating, two matrix inversions and one Cholesky decomposition are involved. A closer observation reveals that the symbol-wise filter updating is solely due to the dependence on the second-order *a priori* information $\mathbf{\Phi}_{n,k}$. Therefore, the computational complexity can be reduced significantly by replacing $\mathbf{\Phi}_{n,k}$ with $\mathbf{\Phi}$, which leads to constant filter matrices, $\mathbf{W}$ and $\mathbf{B}$, for all symbols in the block. It is verified by both simulation and data processing that employing constant filter matrices for all symbols doesn't apparently degrade the equalization performance.

The proposed *sequence-based* equalization gleans bit reliability information from the whole sequence $\mathbf{r}_{n,k}$ (or equivalently, $\tilde{\mathbf{s}}_{n,k}$), rather than the single symbol $\tilde{s}_{n,k}$ used by the *symbol-based* iterative equalization, it thus achieves better performance. The *sequence-based* LLR calculation is more computationally intensive. However, the evaluation can be simplified by utilizing the sparse structure of the equivalent channel matrix $\mathbf{G}_{n,k}$. Details are referred to [16] for SISO systems, and similar results apply to MIMO systems. Generally, the proposed equalization has the same order of computational complexity as the *symbol-based* iterative equalizations in each iteration, while gains more overall computational savings due to its faster converges.

IV. Experimental Results

The proposed iterative receiver using MIMO BDFE was tested by two undersea trials of UWA communications. The first trial named SPACE08, was conducted at the coast of Martha's Vineyard, Edgartown, MA, in October 2008. The second trial named GOMEX08, was conducted at the Gulf of Mexico, in July 2008. Details on the detections of real data are presented in the following two subsections.

A. Results of SPACE08 experiment

In this experiment, the symbol rate was 9.765625 kilo-symbols per second. The carrier frequency was 13 kHz. Modulation schemes included QPSK, 8PSK and 16QAM. The water depth was about 15 meters. The transmitting equipment consisting of four transducers located about 4 meters above the sea bottom. The receiving equipment consisted of six hydrophone arrays, denoted as S1 (60 m, Southeast), S2 (60 m, Southwest), S3 (200 m, Southeast), S4 (200 m, Southwest), S5 (1 km, Southeast) and S6 (1 km, Southwest), respectively. All received files contain 12 channels of data named after their corresponding receiving arrays.

Fig. 4 depicts one transmission frame, which contains the head linear frequency modulation (LFM) signal named LFMB, three packets with QPSK, 8PSK and 16QAM modulations, and the tail LFM signal named LFME. The LFMB and LFME signals aim for the frame (and packet) coarse synchronization and the channel length measurement. Each packet is made up of a *m*-sequence of length 511, and the data payload consists

$$\rho_{n,k}^{j}=\begin{cases} r_j-\sum_{l=j}^{NK} g_{j,l}\left[\hat{s}^{(i)}_{p(l),q(l)}-\bar{s}_{p(l),q(l)}\right], & J<j\le NK,\\ r_J-g_{J,J}s^{(i)}_{n,k}-\sum_{l=J+1}^{NK} g_{J,l}\left[\hat{s}^{(i)}_{p(l),q(l)}-\bar{s}_{p(l),q(l)}\right], & j=J,\\ r_j-g_{j,J}s^{(i)}_{n,k}-\sum_{l=j}^{J-1} g_{j,l}\left[\hat{s}^{(i-1)}_{p(l),q(l)}-\bar{s}_{p(l),q(l)}\right]-\sum_{l=J+1}^{NK} g_{j,l}\left[\hat{s}^{(i)}_{p(l),q(l)}-\bar{s}_{p(l),q(l)}\right], & 1\le j<J. \end{cases} \tag{11}$$

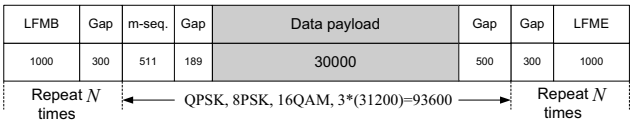

Fig. 4. Frame structure.

of 30,000 modulation symbols. The *m*-sequence plays similar role as LFM signal. The data payload consists of both training blocks and information blocks, with no gaps among blocks. The block size is designated during detection, depending on the channel condition. The placement of training blocks is also flexible, depending on the tradeoff during detection.

The iterative receiver applied to experimental packet detection is described as follows. As mentioned above, the received signal was artificially partitioned into blocks with small time durations. We chose the block size as $N_b = 200$. The MIMO channel with measured channel length of $L = 100$, was estimated either in training mode or in decision-directed (DD) mode. In training mode, the channel was estimated with three training blocks (or $N_p = 600$ training symbols), inserted in the data payload for every T blocks, where T was properly selected so that tradeoff between the detection performance and the training overhead was achieved. In DD mode, $N_p = 600$ previously detected symbols are used to re-estimate the channel, for equalizing the current block. To apply BDFE presented in Section III-A, the post-cursor effect from previous block was removed from the current block, using the equalized soft-decision symbols and the estimated channel. To account for the signal-to-noise ratio (SNR) degradation in the equalized symbols at the tail of current block [14], overlapped block detection was used, for which some equalized symbols at the tail of current block was detected again in the next block. During the detection, we selected an overlapping length of $N_{\text{ovlp}} = 50$ which was conservative since shorter overlapping length still worked well. The percentage of the training overhead could be roughly estimated as $\eta = \frac{N_p}{T(N_b - N_{\text{ovlp}})} \times 100\%$.

Fig. 5 shows an example of the estimated channel impulse responses (CIRs) for the 200 m two-transducer QPSK transmissions. It is obvious from the figure that the subchannels are sparse and some are non-minimum phase, which imposes difficulty on robust UWA communication.

The scatter plots in Fig. 6 and Fig. 7 show the soft-decision symbols at the outputs of the equalizer and the MAP decoder for QPSK and 8PSK, respectively. The improvement over

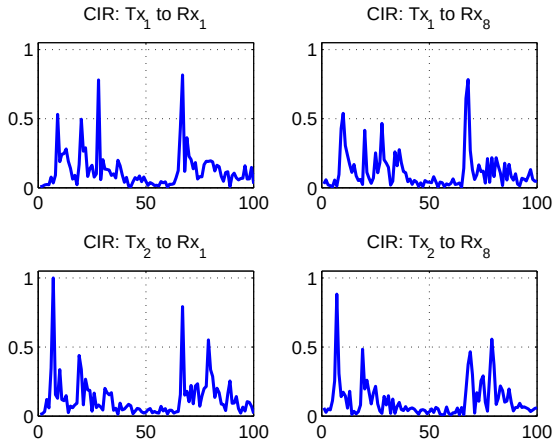

Fig. 5. Estimated channel impulse responses for QPSK transmission.

iterations is clearly observed by comparing subfigures in each row of both figures. The performance improvement after MAP decoder is also observed by comparing subfigues in each column of both figures.

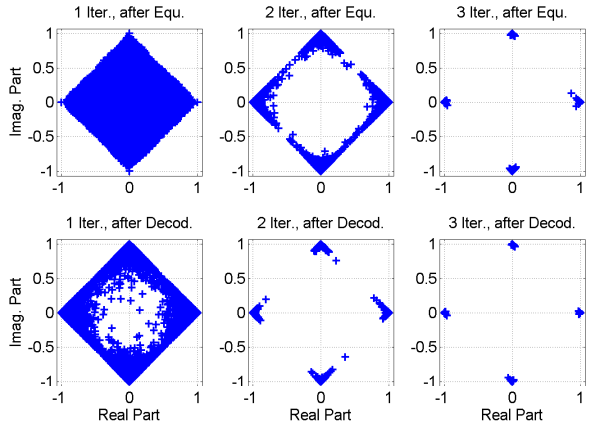

Fig. 6. Soft-decision symbols at the outputs of the soft-decision equalizer and the MAP decoder for QPSK modulation.

For 200 m transmission, 45 packets (30 S3 packets and 15 S4 packets) were processed. The results for the two-transducer QPSK transmission are listed in Table I, where $T = 30$ is selected, incurring the training overhead of 14%. All 45 packets achieve zero bit error rates (BERs), for which most

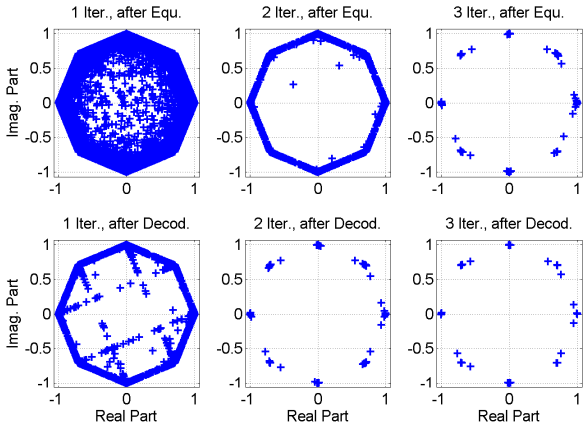

Fig. 7. Soft-decision symbols at the outputs of the soft-decision equalizer and the MAP decoder for 8PSK modulation.

TABLE I
RESULTS FOR 2×12 MIMO 200 M QPSK TRANSMISSION

Number of iterations to achieve zero BER	Number of packets
1	20
2	15
3	6
4	4

packets only require two iterations. For the two-transducer 8PSK transmission, 25 out of 45 packets achieve zero BERs within five iterations. The average BERs for remaining 20 packets are 5.657×10^{-4} and 6.018×10^{-4}, respectively, for the first transducer and the second transducer. The results for the 1000 m, two-transducer, QPSK transmission are listed in Table II, where $T = 20$ incurring 20% training overhead, is selected. All 15 processed packets (5 S5 packets and 10 S6 packets), achieve zero BER after three iterations. For 8PSK case, we get 5 packets achieving zero BERs within three iterations, and the average BER for the remaining 10 packets are 8.024×10^{-5} and 1.191×10^{-3} for the first transducer and the second transducer, respectively.

We next demonstrate the results for the 1000 m three-transducer and four-transducer QPSK transmissions. The BER results are listed in Table III and Table IV, with the training overhead being 24% and 34.7%, respectively. For both cases, zero BERs are achieved after three iterations.

TABLE II
RESULTS FOR 2×12 MIMO 1000 M QPSK TRANSMISSION

Number of iterations to achieve zero BER	Number of packets
1	9
2	5
3	1

TABLE III
BER OF 3×12 MIMO 1000 M QPSK TRANSMISSION

Transducer	Iter. 1	Iter. 2	Iter. 3	Iter. 4
1	9.333e-4	0	0	0
2	3.053e-2	2.333e-4	0	0
3	8.927e-2	1.800e-3	0	0

TABLE IV
BER OF 4×12 MIMO 1000 M QPSK TRANSMISSION

Transducer	Iter. 1	Iter. 2	Iter. 3	Iter. 4
1	1.318e-3	0	0	0
2	1.600e-2	1.364e-4	0	0
3	6.577e-2	1.455e-3	0	0
4	1.100e-2	0	0	0

B. Results of GOMEX08 experiment

In this experiment, a moving transmitting equipment and a fixed receiving equipment was deployed. The transmitting equipment consisted of four transducers located about 50 m deep in the sea at zero speed, and rose to 30 m at high speed of 2.7 knots. The receiving equipment consisted of eight hydrophones was fixed 50 m deep in the sea. The transmission distance was 1.7 km to 2 km and the symbol rate was 4 kilo-symbols per second. The carrier frequency was 17 kHz. Each transmission frame consisted of multiple packets. The number of packets within one frame was 48, 24 and 12 corresponding to the different packet sizes of 1024, 2048 and 4096. The channel length was measured as $L = 80$ in this trial, and a block size of $N_b = 150$ was adopted during detection. The overlapping length was selected as $N_{\text{ovlp}} = 40$. An example of the estimated channel is demonstrated in Fig. 8, where the sparseness and non-minimum phase of the sub-channels are observed, similar to Fig. 5.

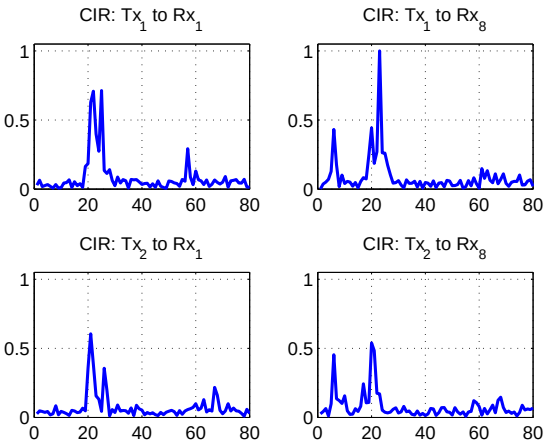

Fig. 8. Estimated channel impulse responses for GOMEX08 experiment.

We present the detection results for three frames with packet size 2048 and three frames with packet size 4096, both with QPSK modulations. The number of iterations required for achieving zero-BER for each packet, are listed in Table V and

TABLE V

NUMBER OF ITERATIONS FOR ACHIEVING ZERO BER: 2×8 MIMO QPSK TRANSMISSION WITH PACKET SIZE 2048

Index of packet	Frame 1	Frame 2	Frame 3
1	1	1	1
2	2	1	2
3	1	1	1
4	1	1	1
5	1	1	1
6	1	1	1
7	2	1	1
8	1	1	1
9	1	1	2
10	1	1	3
11	1	3	1
12	1	2	1
13	1	1	1
14	1	1	1
15	1	1	3
16	1	1	3
17	1	1	1
18	1	4	1
19	1	1	1
20	1	1	1
21	2	1	1
22	1	1	1
23	1	1	1
24	1	2	1

TABLE VI

NUMBER OF ITERATIONS FOR ACHIEVING ZERO BER: 2×8 MIMO QPSK TRANSMISSION WITH PACKET SIZE 4096

Index of packet	Frame 1	Frame 2	Frame 3
1	4	1	1
2	2	2	1
3	1	3	1
4	1	2	1
5	4	2	2
6	3	1	5
7	1	1	3
8	4	1	2
9	2	3	2
10	1	3	1
11	1	1	2
12	3	2	1

Table VI. From both tables, most of the packets require no more than three iterations to achieve zero BER, which again verify the robustness and fast convergence of the proposed turbo receiver.

V. CONCLUSION

We have demonstrated a new receiver structure for high-rate UWA communications, using iterative MIMO BDFE. The proposed soft-decision MIMO BDFE has performed successive interference cancelation of both ISI in the time domain and MI in the space domain, and it has enabled a *sequence-based* LLR calculation leading to excellent detection performance with fast convergence. The MIMO channel has been estimated and tracked relying on either training symbols or previously detected symbols. Rigorous testing of the proposed receiver scheme by extensive experimental data collected in the SPACE08 and GOMEX08 undersea trials, has shown that consistent reliable detection was achieved with moderate training overhead.

ACKNOWLEDGMENTS

This work was supported in part by the National Science Foundation under Grants ECCS-0846486, CCF-0832833 and CCF-0915846, and the Office of Naval Research under Grants N00014-07-1-0219 and N00014-09-1-0011. The work of T. C. Yang was supported by the Office of Naval Research. We thank Dr. James Preisig and his team for conducting the SPACE08 experiment. We are also grateful to Dr. Jingxian Wu for helpful discussion.

REFERENCES

[1] M. Stojanovic, J. Catipovic, and J. Proakis, "Phase-coherent digital communicaitons for underwater acoustic channels," *IEEE J. Ocean Eng.*, vol.19, pp.100-111, Jan. 1994.

[2] Y. R. Zheng, C. Xiao, T.C. Yang, and W.B. Yang, "Frequency-Domain channel estimation and equalization for single carrier underwater acoustic communications," in *Proc. Oceans'07*, Vancouver, 2007.

[3] M. Stojanovic, "Low complexity OFDM detector for underwater acoustic channels," in *Proc. Oceans'06*, 2006.

[4] B. Li, S. Zhou, M. Stojanovic, and L. Freitag, "Pilot-tone based ZP-OFDM demodulation for an underwater acoustic channel," in *Proc. Oceans'06*, 2006.

[5] T. C. Yang, "Correlation-based decision-feedback equalizer for underwater acoustic communications," *IEEE J. Ocean Eng.*, vol.30, pp.865-880, Oct. 2005.

[6] J. Tao, Y. R. Zheng, T. C. Y. C. Xiao, and W.-B. Yang, "Time-domain receiver design for MIMO underwater acoustic communications," in *Proc. Oceans'08*, Quebec City, Canada, Sept. 15-18, 2008.

[7] S. Roy, T. M. Duman, V. McDonald, and J. Proakis, "High rate communication for underwater acoustic channels using multiple transmitters and space-time coding: receiver structures and experimental results," *IEEE J. Ocean. Eng.*, vol.32, pp.663-688, July 2007.

[8] C. Douillard, M. Jezequel, C. Berrou, A. Picart, P. Didier and A. Glavieux, "Iterative correction of intersymbol interference: turbo-equalization," *Eur. Trans. Telecomm.*, vol. 6, pp. 507-511, Sept.-Oct. 1995.

[9] E. Sozer, J. Proakis and F. Blackmon, "Iterative equalization and decoding techniques for shallow wateracoustic channels" in *Proc. MTS/IEEE Oceans'01*, Nov. 2001, vol. 4, pp. 2201-2208

[10] F. Blackmon, E. Sozer and J. Proakis, "Iterative equalization, decoding, and soft diversity combining for underwater acoustic channels," in *Proc. MTS/IEEE Oceans'02*, Oct. 2002, vol. 4, pp. 2425-2428

[11] M. Tuchler, R. Koetter and A. C. Singer, "Turbo equalization: principles and new results," *IEEE Trans. Commun.* vol. 50, pp. 754-767, May 2002.

[12] J. F. Sifferlen, H. C. Song, W. S. Hodgkiss, W. A. Kuperman, and J. M. Stevenson, "An iterative equalization and decoding approach for underwater acoustic communication," *IEEE J. Ocean Eng.*, vol. 33, no. 2, pp. 182-197, April 2008

[13] R. Otnes, T. H. Eggen, "Underwater acoustic communications: long-term test of turbo equalization in shallow water," *IEEE J. Ocean Eng.*, vol. 33, no. 3, pp. 321-334, July 2008

[14] G. K. Kaleh, "Channel equalization for block transmission systems," *IEEE J. Sel. Areas Commun.*, vol. 13, no. 1, pp. 110-121, Jan. 1995.

[15] L. Bahl, J. Cocke, F. Jelinek, and J. Raviv, "Optimal decoding of linear codes for minimizing symbol error rate," *IEEE Trans. Inform. Theory*, vol. IT-20, pp. 284-287, March 1974.

[16] J. Wu and Y. R. Zheng, "Low complexity soft-input soft-output block decision feedback equalization," *IEEE J. Sel. Areas Commun.*, vol. 26, pp. 281-289, Feb. 2008.